Revista Brasileira de Paleontologia, 24(4):311–322, Outubro/Dezembro 2021
A Journal of the Brazilian Society of Paleontology

doi:10.4072/rbp.2021.4.02

REVISION OF MIDDLE DEVONIAN CONODONT BIOSTRATIGRAPHY IN THE NEGHELEH SECTION, CENTRAL IRAN

HOSSEIN GHOLAMALIAN
Department of Geology, Faculty of Sciences, University of Hormozgan, Po. Box 3995, Bandar Abbas, I.R. Iran.
hossein_gholamalian@yahoo.com (corresponding author)

VACHIK HAIRAPETIAN
Department of Geology, Islamic Azad University, Khorasgan (Esfahan) Branch, Esfahan, I.R. Iran.
vachik@khuisf.ac.ir

MOHAMMAD POOSTI
Department of Geology, Faculty of Sciences, University of Hormozgan, Po. Box 3995, Bandar Abbas, I.R. Iran.
m.poosti@yahoo.com

ABSTRACT – Fifteen conodont species and subspecies from the Negheleh section, Soh area, north of Esfahan represent early Eifelian to middle Givetian time interval. Five biozones: *costatus* to *australis*, *kockelianus*, *ensensis* to *hemiansatus*, *timorensis* and *rhenanus* to *ansatus* are recognized. The present study suggests the Eifelian age for the base of Bahram Formation in the Sanandaj-Sirjan and the western part of Central Iran Microplate. The oldest known occurrence of thelodont turiinid species, *Neoturinia hutkensis* is reported from the early Eifelian strata of the Negheleh section. New age range from the late Eifelian to late Frasnian is proposed for *Icriodus excavatus* Weddige.

Keywords: Middle Devonian, Eifelian, Givetian, conodonts, biostratigraphy.

RESUMO – Quinze espécies e subespécies de conodontes da seção Negheleh, área de Soh, ao norte de Esfahan representam o intervalo de tempo Eifeliano inferior a Givetiano médio. Cinco biozonas: *costatus* a *australis*, *kockelianus*, *ensensis* a *hemiansatus*, *timorensis* e *rhenanus* a *ansatus* são reconhecidas. O presente estudo sugere a idade Eifeliana para a base da Formação Bahram em Sanandaj-Sirjan e na parte ocidental da Microplaca Central Iraniana. A ocorrência mais antiga conhecida da espécie turiinidae thelodonte, *Neoturinia hutkensis*, é relatada nos estratos eifelianos da seção Negheleh. Uma nova faixa de idade do Neoeifeliano ao Neofrasniano é proposta para *Icriodus excavatus* Weddige.

Palavras-chave: Devoniano Médio, Eifeliano, Givetiano, conodontes, bioestratigrafia.

INTRODUCTION

Among the Middle Devonian studies of Central Iran and Sanandaj-Sirjan terrane, there are a few well documented works on conodonts and brachiopods (*e.g.* Nasehi, 1997, 2018; Brice *et al*., 2006) in strata dated as pre-Givetian. The Negheleh section in the Soh area, East of the Sanandaj-Sirjan terrane with prolific Eifelian–Givetian beds is selected for conodont biostratigraphy (Figure 1). This section is located in the Soh area, 98.5 km North of Esfahan, central Iran, and can be accessed via a 15 km long gravel road (Figure 1). Coordinates for the base of the section are: 33˚28'46.25''N, 51˚35'20.04''E. Biozonation of the Eifelian and Givetian strata and revision of the previous works are the aims of this paper.

GEOLOGICAL FRAMEWORK

The studied area in the Soh region is located in the eastern margin of the Sanandaj-Sirjan tectono-stratigraphic terrane (Figure 1). The presence of basic igneous and metamorphic bodies is an important characteristic of this area. The Silurian sequence is the oldest exposed stratigraphic unit and consists of red sandstones with thick basaltic lavas (Figure 2). Devonian strata have been recorded for the first time by Zahedi (1973) as the Padeha and Bahram formations. The ?Early to Middle Devonian (?Lochkovian to Eifelian) Padeha Formation beds are composed of pink sandstones and mudstones that conformably underly the Middle to Late Devonian (Eifelian to Frasnian) Bahram Formation strata. The Late Devonian terrigenous interval composed of refractory

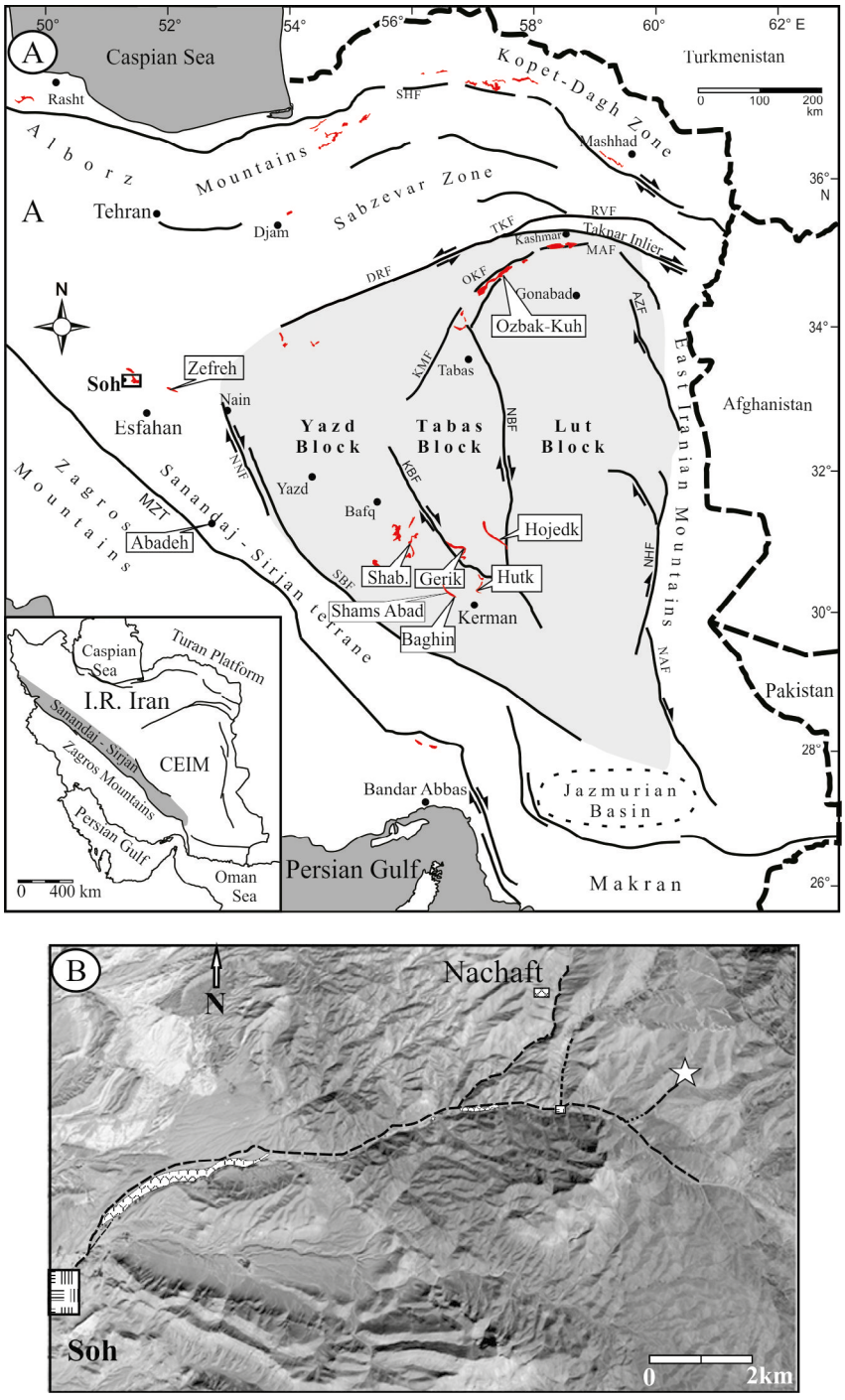

Figure 1. A, map of Iran with location of the studied area in the East of the Sanandaj-Sirjan terrane (structural map of Central Iran after Hairapetian *et al.*, 2017). Locality of some of Devonian outcrops are shown in red. These sections are studied by Yazdi *et al.* (2000), Ashouri (2004), Brice *et al.* (2006), Gholamalian (2006), Gholamalian & Kebriaei (2008), Gholamalian *et al.* (2011, 2013, 2014). **B**, road map of Soh area with locations of Negheleh and Nachaft sections. White asterisk shows the location of Negheleh section (present study). **Abbreviations: AZF**, Abiz Fault; **DRF**, Doruneh Fault; **KBF**, Kuhbanan Fault; **KMF**, Kalmard Fault; **MAF**, Mehdi-Abad Fault; **MZT**, Main Zagros Thrust; **NAF**, Nostrat-Abad Fault; **NBF**, Nayband Fault; **NHF**, Nehbandan Fault; **NNF**, Nain Fault; **OKF**, Ozbak Kuh Fault; **RVF**, Rivash Fault; **SBF**, Shahr-e-Babak Fault; **Shab.**, Shabjereh section; **SHF,** Siah Kuh Fault; **TKF**, Taknar Fault.

argillite clays can be seen in the entire study area (Figure 2). A major hiatus representing most of the Late Devonian and Carboniferous is another characteristic of this area (Zahedi, 1973; Ghobadi Pour *et al*., 2013).

LITHOSTRATIGRAPHY

Devonian strata of the Central Iran and Sanandaj-Sirjan zones are traditionally devided into the terrigenous Padeha

Formation and the carbonates of the Sibzar, Bahram and Shishtu formations. The Early to Middle Devonian age of the Padeha Formation is mostly based on its stratigraphic position and very few paleontological data *e.g.* Nasehi (1997) who attributed it to the Lochkovian to Givetian based on conodonts. Nasehi (2018) recently revised his idea and proposed a Pridoli to Givetian age for the Padeha Formation. The age of the Sibzar and Bahram formations has also been determined by more precise studies, especially the ones based on conodont biostratigraphy in the Tabas, Kerman and Abadeh areas (Yazdi, 1999; Yazdi *et al*., 2000; Ashouri, 2004; Wendt *et al*., 2002, 2005; Gholamalian & Kebriaei, 2008; Gholamalian *et al*., 2009, 2011, 2013). These studies show a late Givetian to early Frasnian age for the base of Bahram Formation in the mentioned areas. However, there are older strata of the Bahram Formation in some sections in the Sanandaj-Sirjan and western Central Iran zones (Soh and Zefreh areas) that have a confirmed Early Eifelian to Givetian age (Brice *et al*., 2006). Meanwhile Bahrami *et al*. (2015, 2018) and Königshof *et al*. (2017) incorrectly attributed all of these strata to the late Givetian (*expansus* and *subterminus* zones) without any attention to the exact ranges of conodont species. For example, they accomodated *Icriodus arkonensis wallisierianus* and *Polygnathus ensensis* in the *expansus* Zone (Bahrami *et al*., 2015, Figure 3). But we suppose the range of *ensensis–rhenanus/vacus* zones for this association. In many sections, such as Hutk, Hojedk and Baghin (Kerman area) and Negheleh and Nachaft (Soh area), the Bahram Formation

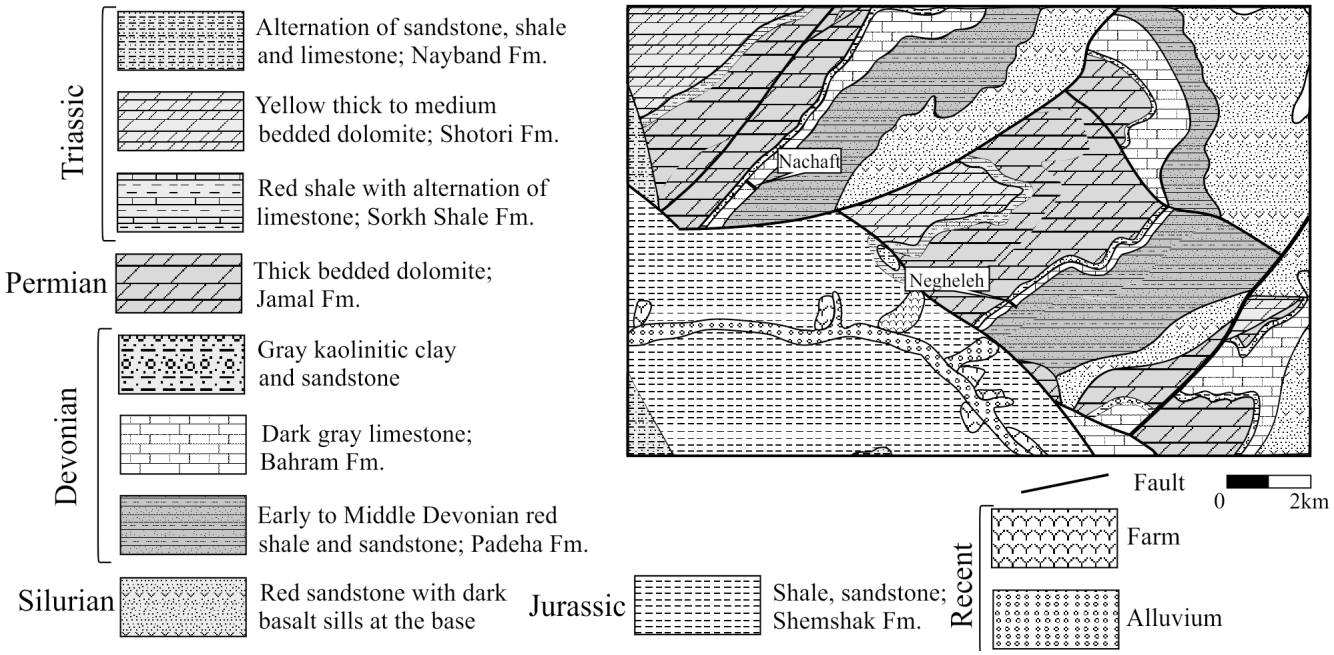

Figure 2. Geological map of studied area, redrawn from Zahedi (1973). Locations of Negheleh (present study) and Nachaft sections are indicated.

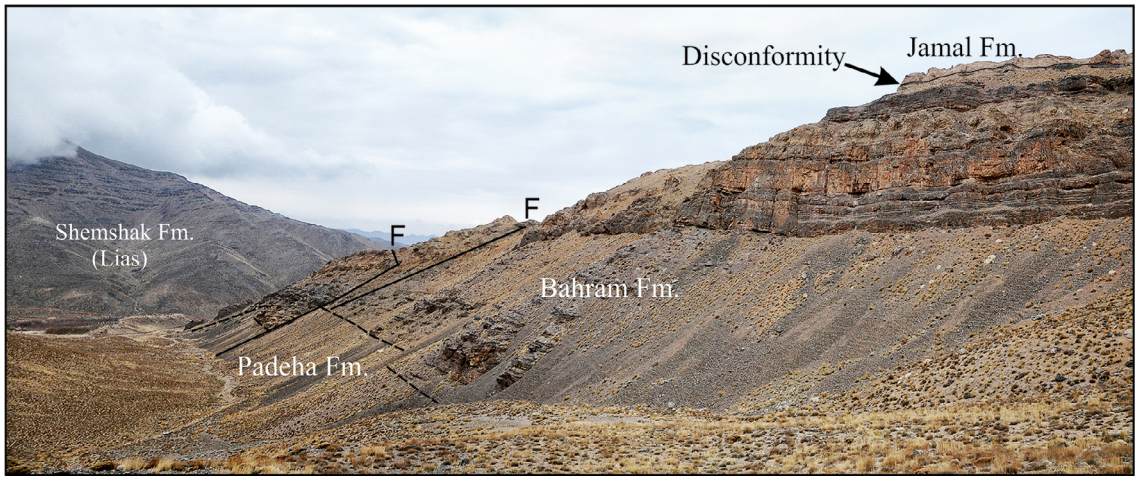

Figure 3. General view of the lithostratigraphic units in the Negheleh section. Disconformity between the Devonian strata and the Permian Jamal Formation is indicated by the black arrow.

directly overlies the top of the Padeha Formation showing the lateral change of the Sibzar Formation dolomites to the basal Bahram Formation limestones. The base of the Bahram Formation seems to be diachronous; Eifelian in Negheleh (present work) and Zefreh (Brice *et al*., 2006), late Givetian in the most of Kerman area sections (Gholamalian *et al*., 2013) and Famennian in the Shams-Abad, west of Kerman (Bahrami *et al*., 2011). Therefore, it seems that the oldest Devonian carbonate sequences of Iran can be observed in the Soh area (Sanandaj-Sirjan terrane), in the western margin of the Central-East Iran Microplate (**CEIM**).

STUDIED SECTION

The base of the Bahram Formation carbonates of the studied succession conformably overlies the sandstones of the top of the Padeha Formation and starts with 60 cm of thin bedded calcareous dolostone and one meter of brecciated dolomitic limestone (including thelodont scales at the base) (Figure 4). The succession continues with 21.3 m of calcareous dolostone. The main part of the stratigraphic section is composed of 72.7 m of medium bedded limestone that is disconformably overlain by 1.7 m of early Frasnian fossiliferous kaolinitic refractory clay beds. Ghobadi Pour *et al*. (2013) have described early Frasnian (Lower *falsiovalis* Zone) trilobites and brachiopods from similar beds in the upper part of the Nachaft section, 10 Km NW of Negheleh (Figure 1). It seems that the late Givetian beds are eroded in this section. The Permian Jamal Formation also disconformably overlies the top of the refractory clay interval, and shows a major hiatus spanning from the early Frasnian to the Late Carboniferous (Figure 5). This hiatus may be the result of the Hercynian epeirogenesis.

MATERIAL AND METHODS

For the research presented here, 36 samples (each 3–4 kg) were taken from the Negheleh section and dissolved in buffered glacial acetic acid. Twenty three samples were somewhat productive and contain 15 species and subspecies belonging to three genera (Table 1, Figure 6). Samples were proccessed in the laboratory of paleontology, University of Hormozgan. All specimens are stored in the museum of geology, University of Hormozgan under repository codes **HUIC** and **HUIF**.

BIOSTRATIGRAPHY

Polygnathid and icriodid fauna allowed us to use the Middle Devonian standard zones of Weddige (1977) and the later revised biozonations of Klapper & Johnson (1980, 1990) and Belka *et al*. (1997). Standard zones of Klapper (1989) and Ziegler and Sandberg (1990) are occasionally used for the Frasnian strata (Figure 6). Thelodont scales are associated with icriodid species at the base of the section (sample GSA) (Figure 6).

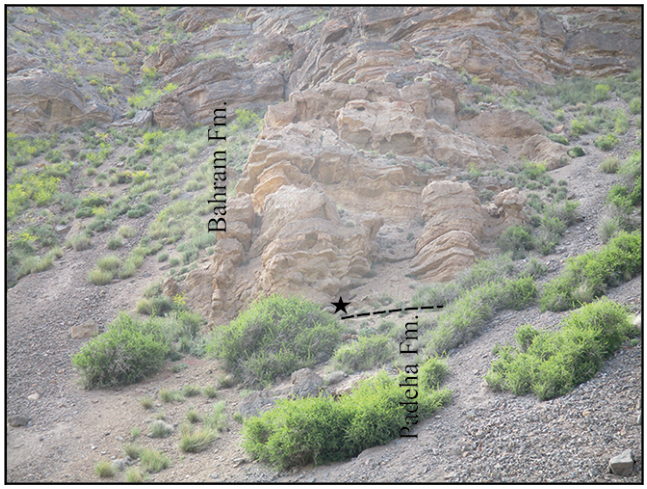

Figure 4. The lower part of Bahram Formation in the Negheleh section with yellow limey dolomite. Asterisk shows the turiniid fish bed (sample GSA) at the base.

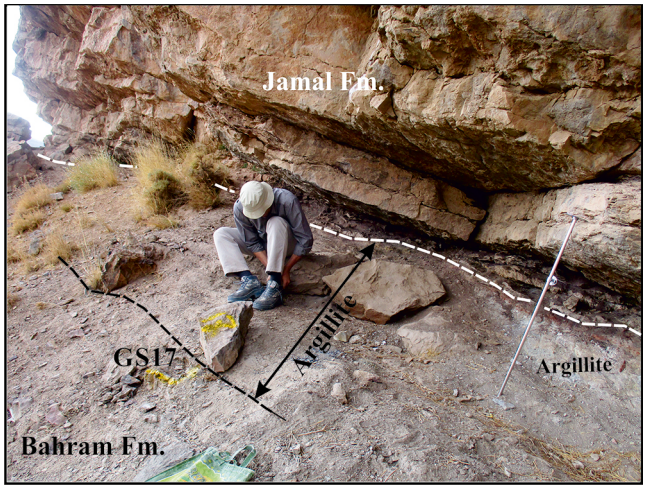

Figure 5. Contacts between Bahram Formation, fireclay interval and Jamal Formation at the top of section. Disconformity between Devonian and Permian strata is indicated by the white line.

***costatus–australis* zones**. The base of this zone is determined by the first appearance datum of *Icriodus regularicrescens* ranging from the *costatus* to the *timorensis* zones (Bultynck, 2003; Gouwy *et al*., 2013). Belka *et al*. (1997) have also reported the first occurrence of this species in the *costatus* Zone of eastern Anti-Atlas sections, Morocco. Gouwy *et al*. (2016) reported this species from the *costatus* Zone of the Central Pyrenees, Spain.

Sixty-three scales of *Neoturinia hutkensis*, associated with *Icriodus regularicrescens* in sample GSA, are the oldest known specimens of this species to date (Figure 6). This species has formerly been reported from early Givetian to early Frasnian (*hemiansatus–hassi* zones) (Hairapetian *et al*., 2016), although an older occurrence within the Eifelian has also been recorded.

***kockelianus* Zone.** The base of this zone is recognized by the first appearance of *Polygnathus linguiformis saharicus*

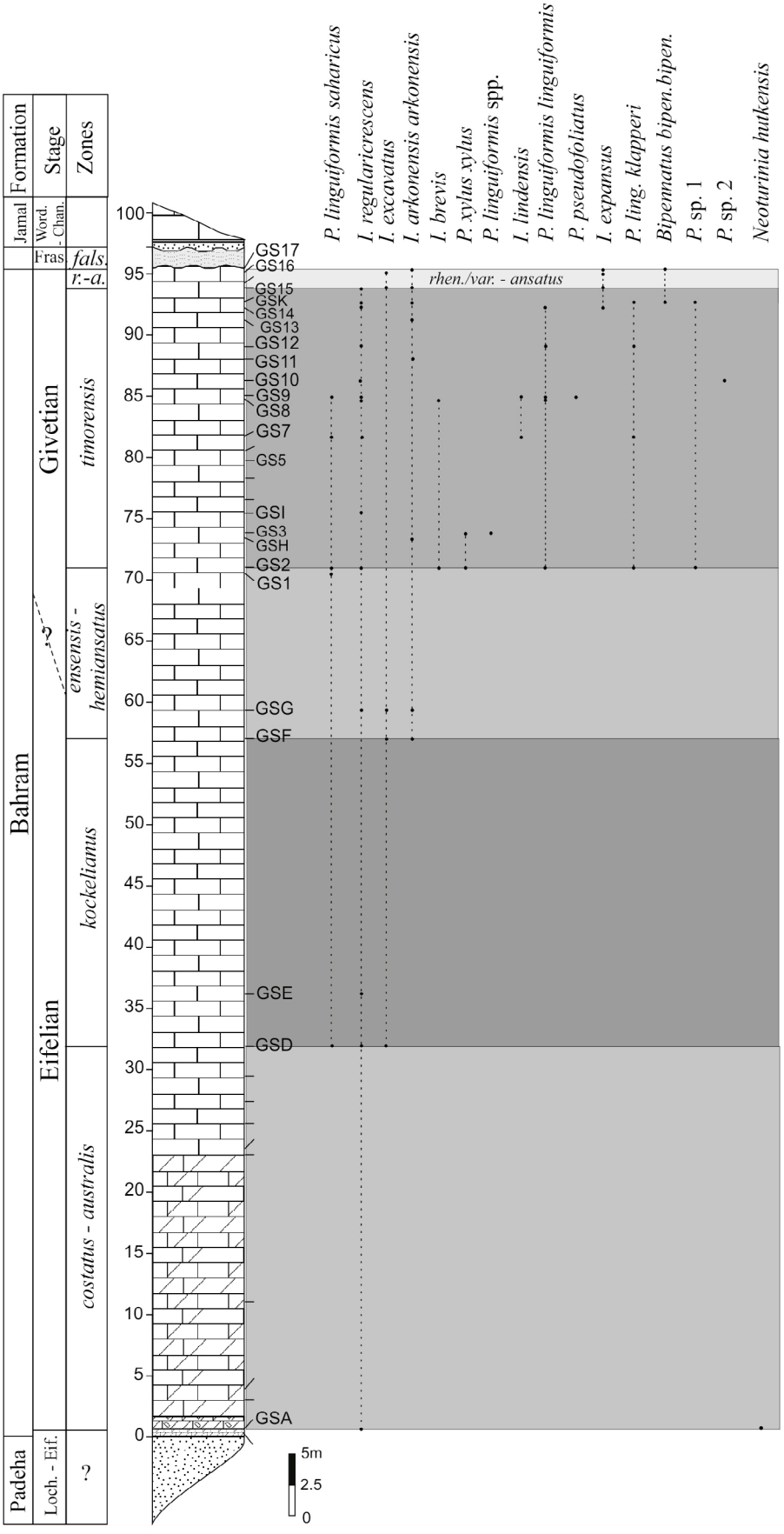

Figure 6. Stratigraphic column, distribution of conodont species and biozonation of the Negheleh section. **Abbreviations: *r.-a.***, *rhenanus/ansatus*; ***fals.***, *falsiovalis*; **Loch.–Eif.**, Lochkovian–Eifelian.

(Figure 6, Figures 7Y–ZZ, 8A). Other associated species are *Icriodus regularicrescens* and *I. excavatus*. According to Narkiewicz & Königshof (2018), *P. linguiformis saharicus* ranges from the *kockelianus* to *ansatus* zones. The upper limit of the present zone is coincident with the base of the next interval.

The first appearance datum of *Icriodus excavatus* that was previously recorded from the *rhenanus/varcus* Zone (Belka *et al*., 1997; Narkiewicz & Bultynck, 2007) occurs here (Figures 6, 7K–L, 7N). Gholamalian & Kebriaei (2008) extended the last appearance datum of this species to the Upper *rhenana* Zone of the Frasnian of the Hojedk section, Kerman area. So, by composing these data from the Negheleh and Hojedk sections, we can propose a more extended range from the *kockelianus* to Upper *rhenana* zones for *I. excavatus*.

***ensensis–hemiansatus* zones.** The base of this zone is identified by the entry of *Icriodus arkonensis arkonensis*. According to Belka *et al*. (1997) and Narkiewicz & Bultynck (2007), this species ranges from the *ensensis* to the *ansatus* zones. Other associated species are *I. excavatus* and *I. regularicrescens*. The present interval encompasses the Eifelian/Givetian boundary, but we cannot precisely identify it due to the absence of *Polygnathus hemiansatus* as the basal Givetian index species (Walliser *et al*., 1995).

***timorensis* Zone.** The lower limit of this zone is recognized by the entry of *Polygnathus xylus xylus* and *Icriodus brevis* at the base of *timorensis* Zone (Barskov *et al*., 1991; Narkiewicz & Bultynck, 2007). Other species of this interval are: *I. arkonensis arkonensis*, *I. regularicrescens*, *I. lindensis*, *I. expansus*, *P. linguiformis linguiformis*, *P. linguiformis saharicus*, *P. linguiformis klapperi*, *P. linguiformis* spp., *P. pseudofoliatus*, *P.* sp. 1 (Figures 7C–J, 7R–S, 7T–ZZ, 8B–D, 8E, 8F). *Icriodus lindensis* that ranges from *hemiansatu*s to *ansatus* zones (Bultynck, 2003) also occurs here. The upper limit of this zone is recognized by the last appearance of *I. regularicrescens*.

***rhenanus* to *ansatus* zones.** The lower and upper limits of this zone are coincident with the top of the previous zone and the last occurrence of *Icriodus arkonensis arkonensis* respectively. Other associated species are: *Icriodus expansus*, *I. excavatus* and *Bipennatus bipennatus bipennatus*.

SYSTEMATIC PALEONTOLOGY

Order PRIONIODONTIDA Dzik, 1976
Family ICRIODONTIDAE Müller & Müller, 1957

Icriodus Branson & Mehl, 1938

Type species. *Icriodus expansus* Branson and Mehl, 1938.

Icriodus arkonensis arkonensis Stauffer, 1938
(Figures 7C–F)

Material. 51 specimens from multiple samples, see Table 1.

Table 1. Distribution chart and biozonation of conodonts in the Negheleh section, Central Iran. **Abbreviation: *rhen/var.*** = *rhenanus/varcus*.

Biozones	*costatus - australis*	*kockelianus*		*ensensis - hemiansatus*				*timorensis*												*rhen/var. - ansatus*	
Species	GSA	GSD	GSE	GSF	GSG	GS1	GS2	GSH	GS3	GSI	GS5	GS7	GS8	GS9	GS10	GS11	GS12	GS13	GS14	GSK	GS15	GS16	GS17
P. linguiformis saharicus		▲3				2	5					1		1									
Icriodus regularicrescens	▲ 1	3	1		3		6			2		3	2	2	1		4		1	4	1▼		
I. excavatus		19		1	3																1	2	
I. arkonensis arkonensis				▲29	10			2								1		1		1	3		4▼
I. brevis							▲1																
P. xylus xylus							▲3																
P. linguiformis spp.							1		1														
I. lindensis												1		1									
P. linguiformis linguiformis							1						1	2			1						
P. pseudofoliatus														1									
I. expansus																			2		1	1	
P. linguiformis klapperi							1					2					1						
Bipennatus bip. bip.																				1			1
P. sp. 1							1													1			
P. sp. 2															1						1		
Unassigned elements							5			2	1		1										

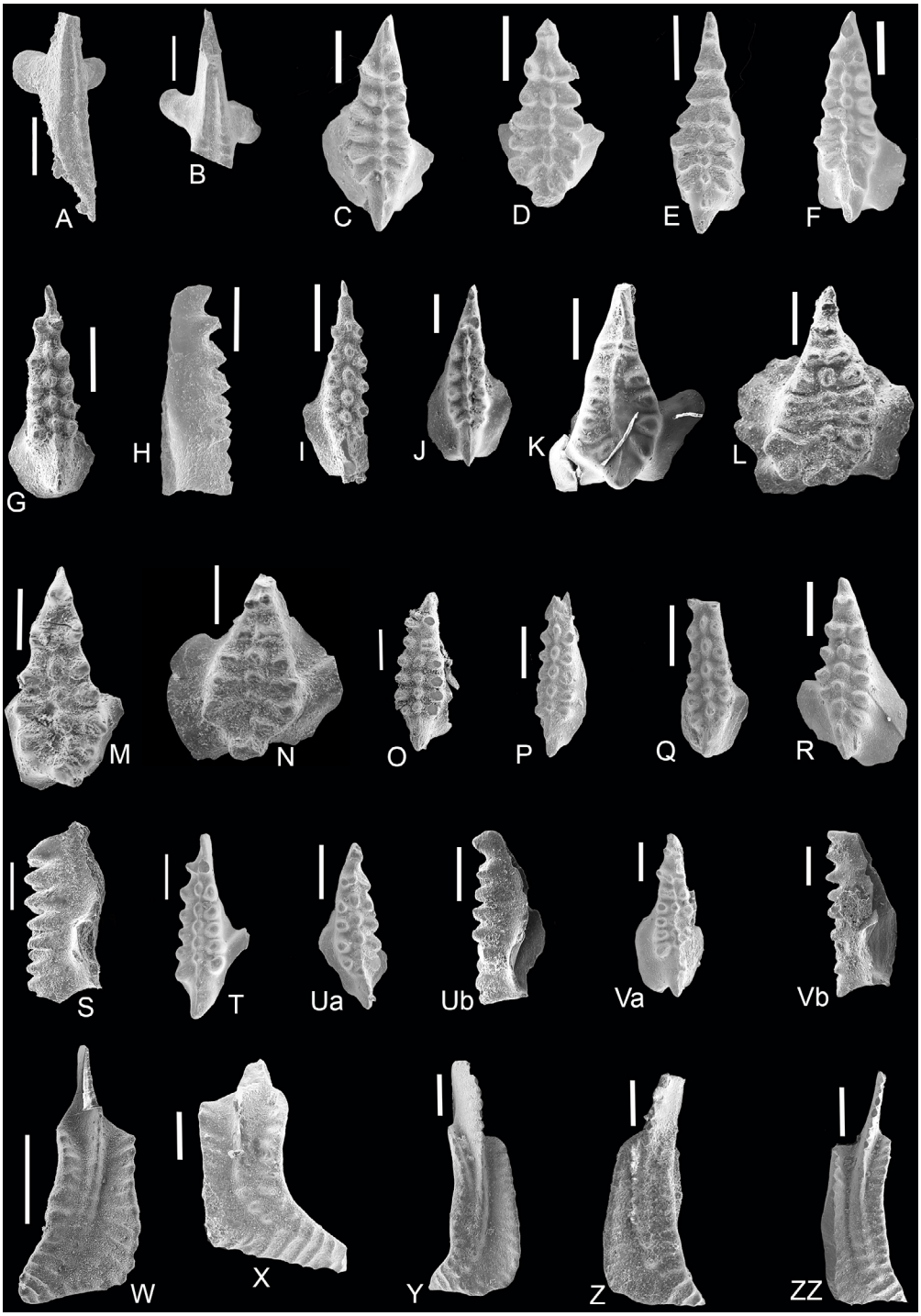

Figure 7. A–B, *Bipennatus bipennatus bipennatus* (Bischoff & Ziegler, 1957), **A**, upper view of HUIC644, sample GS17, Negheleh section; **B**, upper view of HUIC645, sample GSK, Negheleh section. **C–F**, *Icriodus arkonensis arkonensis* Stauffer, 1938, **C**, upper view of HUIC646, sample GS11, Negheleh section; **D**, upper view of HUIC647, sample GSG, Negheleh section; **E**, upper view of HUIC648, sample GSF, Negheleh section; **F**, upper view of HUIC649, sample GS15, Negheleh section. **G–H**, *Icriodus brevis* Stuaffer, 1938, upper and lateral views of HUIC650, sample GS2, Negheleh section. **I–J**, *Icriodus regularicrescens* Bultynck, 1970, **I**, upper view of HUIC651, sample GS8, Negheleh section; **J**, upper view of HUIC678, sample GS12, Negheleh section. **K–N**, *Icriodus excavatus* Weddige, 1984, **K**, upper view of HUIC655, sample GSD, Negheleh section; **L**, upper view of HUIC656, sample GSD, Negheleh section; **M**, upper view of HUIC657, sample GSF, Negheleh section; **N**, upper view of HUIC658, sample GSD, Negheleh section. **O–Q**, *Icriodus expansus* Branson & Mehl, 1938, **O**, upper view of HUIC659, sample GS14, Negheleh section; **P**, upper view of HUIC660, sample GS16, Negheleh section; **Q**, upper view of HUIC661, sample GS17, Negheleh section. **R–S**, *Icriodus lindensis* Weddige, 1977, upper and lateral views of HUIC662, sample GS9, Negheleh section. **T–Vb**, *Icriodus regularicrescens* Bultynck, 1970, **T**, upper view of HUIC652, sample GSK, Negheleh section, **Ua–Ub**, upper and lateral views of HUIC653, sample GSK, Negheleh section; **Va–Vb**, upper and lateral views of HUIC654, sample GS12, Negheleh section. **W**, *Polygnathus linguiformis saharicus* Narkiewicz & Königshof, 2018, upper view of HUIC663, sample GSD, Negheleh section. **X**, *Polygnathus linguiformis linguiformis* Hinde, 1879, upper view of HUIC664, sample GS9, Negheleh section. **Y–ZZ**, *Polygnathus linguiformis saharicus* Narkiewicz & Königshof, 2018, **Y**, upper view of HUIC665, sample GS7, Negheleh section; **Z**, upper view of HUIC666, sample GSD, Negheleh section; **ZZ**, upper view of HUIC667, sample GS2, Negheleh section. Scale bars = 200 µ.

Stratigraphic range. This subspecies ranges from the *ensensis* to the *ansatus* zones (Belka *et al*., 1997; Narkiewicz & Bultynck, 2007).
Description. The figured specimens can be assigned to this subspecies based on the biconvex or tear-shaped (Figure 7E) outline, a medial row composed of 6–8 small rounded denticles that extends to the posterior broad and wide cusp. Oval-shaped lateral denticles with transverse crests connect to the medial row (Figures 7C–E). The medial row denticles are joined by a narrow longitudinal ridge that extends to the posterior end of the spindle.
Remarks. Our specimens of *Icriodus arkonensis arkonensis* are different from *I. arkonensis walliserianus* by having a broader and biconvex platform; and cross-form junction of crests of the lateral denticles to the medial row in the later subspecies.

Icriodus brevis Stauffer, 1940
(Figures 7G–H)

Material. One element from sample GS2.
Stratigraphic range. *timorensis* to Lower *falsiovalis* zones (Narckiewicz & Bultynck, 2007).
Description. The figured specimen of this species can be recognized by having a slender shape with slightly biconvex outline and sharp anterior tip. Five to six circular denticles are present on the medial row. Posterior extension of the middle row is composed of 2–3 partially fused denticles. The cusp is not inclined and has the same height as the other denticles of the spindle.

Icriodus excavatus Weddige, 1984
(Figures 7K–N)

Material. Three specimens from sample GSD, one from GSE, one from GSF, three from GSG, one from GS15 and two from GS16.
Stratigraphic range. *kockelianus*–Upper *rhenana* zones (see *kockelianus* Zone in the biostratigraphy chapter).
Description. The figured specimens of *Icriodus excavatus* are characterized by large size and drop-shape broad biconvex outline. Carina is composed of 5–6 rounded denticles; and extends to a wide depression formed by a smaller middle row denticle, in the posterior part of the spindle. A broad and short posterior cusp (irregularly shaped in some of the figured specimens) is present. Each lateral row is composed of 6-8 oval-shaped denticles. These lateral denticles join the medial ones by thin transverse ridges. Our specimens (Figures 7K–N) are comparable to those of Weddige (1984) in general outline, broad biconvex platform, and ornamentation.

Icriodus regularicrescens Bultynck, 1970
(Figures 7I–J, 7T–Vb)

Material. See Table 1.
Stratigraphic range. This species ranges from the *costatus* to the *timorensis* zones (Bultynck, 2003; Gouwy *et al*., 2013).
Description. Our specimens of this species are slender with parallel to semi-parallel lateral margins and sharp anterior tip. Carina is composed of 7–8 rounded denticles, connected to each other by a narrow longitudinal ridge in some of the specimens. Posterior cusp is horn-shaped and composed 2–3 fused denticles. The cusp is strongly inclined. All denticles have the same height. The lower margin of platform is curved beneath the posterior extension of the middle row.

Order OZARKODINIDA Dzik, 1976
Family POLYGNATHIDAE Bassler, 1925

Polygnathus Hinde, 1879

Type species. *Polygnathus dubius* Hinde, 1879.

Polygnathus linguiformis Hinde, 1879

Polygnathus linguiformis saharicus Narkiewicz & Königshof, 2018
(Figures 7W, 7Y–ZZ, 8A)
Material. Three specimens from sample GSD, two from GS1, five from GS2, one from GS7, and one from GS9.
Stratigraphic range. This subspecies ranges from the *kockelianus* to *ansatus* zones (Narkiewicz & Königshof, 2018).
Description. The figured specimens of this subspecies can be identified by their asymmetrical platform. The anterior part of platform is narrower than the rest. The outer platform becomes broad toward the posterior. The widest part of platform is at the posterior one-third. The outer margin is curved at the connection of platform and tongue. The platform and tongue are ornamented by transverse ridges. Adcarinal troughs are deep in almost the entire platform length and become wide in the posterior part. Carina is fused and high in the anterior part of platform, but gradually becomes low towards the widest part of platform and continues as four separated nodes. It does not reach the posterior tip.

Polygnathus xylus xylus Stauffer, 1940
(Figures 8G–H)

Material. Three elements from sample GS2.
Stratigraphic range. Middle Givetian (*timorensis* Zone) to lower Frasnian (Barskov *et al*., 1991).
Description. The figured specimens of this *Polygnathus* subspecies is identified by the lanceolate shape of the elongate platform with parallel lateral margins. Carina is high and fused, but 3–4 separate denticles can be seen on its posterior half. Adcarinal troughs are deep, narrow and extend to the posterior end. The posterior end of the platform forms a sharp tip. No ornamentation is seen on the platform surface.

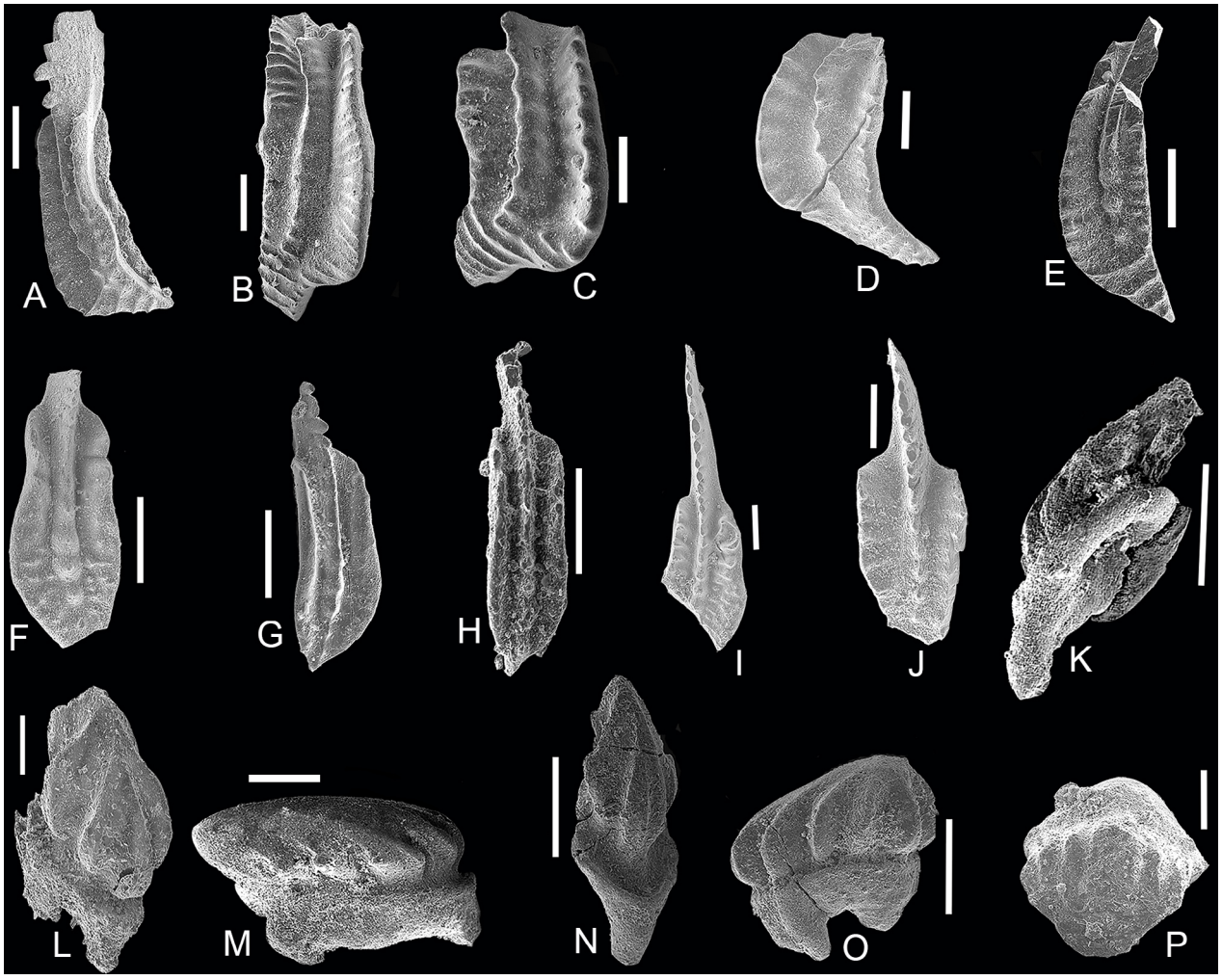

Figure 8. A, *Polygnathus linguiformis saharicus* Narkiewicz & Königshof, 2018, upper view of HUIC668, sample GS2, Negheleh section. **B**–**D**, *Polygnathus linguiformis klapperi* Clausen, Leuteritz & Ziegler, 1979; **B**, upper view of HUIC669, sample GS2, Negheleh section; **C**, upper view of HUIC670, sample GSK, Negheleh section; **D**, upper view of HUIC671, sample GS12, Negheleh section. **E**, *Polygnathus linguiformis* spp., upper view of HUIC672, sample GS2, Negheleh section. **F**, *Polygnathus pseudofoliatus* Wittekindt, 1965, upper view of HUIC673, sample GS9, Negheleh section. **G**–**H**, *Polygnathus xylus xylus* Stauffer, 1940, **G**, upper view of HUIC674, sample GS10, Negheleh section; **H**, *Polygnathus xylus xylus* Stauffer, 1940, upper view of HUIC675, sample GS2, Negheleh section. **I**, *Polygnathus* sp. 1, upper view of HUIC676, sample GS2, Negheleh section. **J**, *Polygnathus* sp. 2, upper view of HUIC677, sample GS10, Negheleh section. **K**–**O**, *Neoturinia hutkensis* (Bleick and Goujet, 1978), **K**, trunk scale in lateral crown view, HUIF1, sample GSA, Negheleh section; **L**, trunk scale in oblique lateral crown view, HUIF2, sample GSA, Negheleh section; **M**, cephalopectoral scale in lateral crown view, HUIF4, sample GSA, Negheleh section; **N**, trunk scale in oblique lateral crown view, HUIF3, sample GSA, Negheleh section; **O**, cephalopectoral scale in lateral crown view, HUIF5, sample GSA, Negheleh section. **P**, *Nostolepis* sp. indet., scale in crown view, HUIF6, sample GSA, Negheleh section. All scale bars are 200 µ except for figures K–P those are 500 µ.

CORRELATION TO THE NACHAFT SECTION

The Nachaft section in the Joor Maadan valley, 10 km northwest of Negheleh was first studied by Adhamian (2003) for conodont biostratigraphy. He found conodonts in 78 m of the middle part of the section and attributed it to the early Givetian *hemiansatus* to Lower *varcus* zones (Figure 9). Subsequently, Ghobadi Pour *et al*. (2013) updated the biozonation of this section and summarized it in *hemiansatus–ansatus* zones. Reconsidering the association of *Icriodus arkonensis arkonensis*, *I. lindensis* and *Polygnathus xylus xylus* that is reported from Nachaft section by Adhamian (2003) and Ghobadi Pour *et al*. (2013) from their beds 38–59 guided us to identify the *ensensis–hemiansatus* and *timorensis–ansatus* zones for the middle part of the Nachaft section (Figure 9).

Rahmati & Yazdi (2008) have recovered *Ancyrodella pristina* (synonym of *An. rotundiloba* in our opinion) and *An. binodosa* from a limestone bed 29 m below the argillite interval of the Nachaft section, suggesting the early Frasnian Lower *falsiovalis* Zone age (MN1 Zone of Klapper, 1989). Therefore the correlation can suggest the early Frasnian age for the argillite interval in the Negheleh sections (Figure 9). Notwithstanding, these refractory (argillite) beds are reported in literature to be diachroneous; Frasnian in the Ozbak-Kuh area and late Frasnian to early Famennian in the Abadeh area (Yazdi *et al*., 2000; Torshizian & Molaei, 2007).

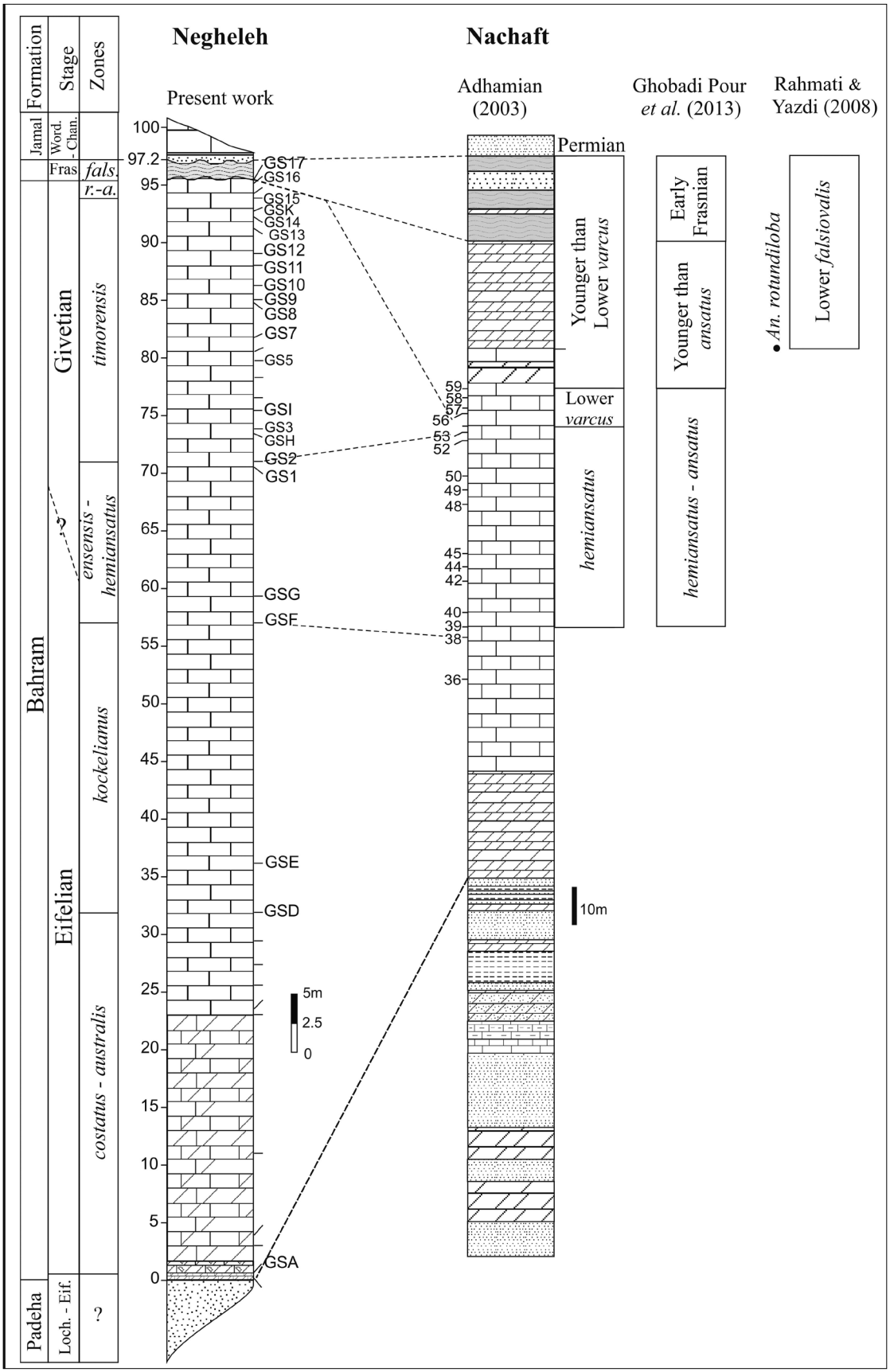

Figure 9. Lithostratigraphic and biostratigraphic correlation between Negheleh (present study) and Nachaft section (Adhamian, 2003; Ghobadi Pour *et al.*, 2013; Rahmati & Yazdi, 2008). **Abbreviations:** ***r.-a.***, *rhenanus/ansatus*; ***fals.***, *falsiovalis*; ***tim.–ans.***, *timorensis–ansatus*; **Loch.–Eif.**, Lochkovian–Eifelian.

CONCLUSIONS

Conodont research at the Negheleh section revealed an early Eifelian to middle Givetian (*costatus* to *ansatus* zones) age for the Bahram Formation. The present conodont research is the first documented report of Eifelian beds from the Sanandaj-Sirjan terrane. The oldest occurrence of the thelodont turiinid species, *Neoturinia hutkensis* has been reported here from the early Eifelian (*costatus–australis* zones) beds. An early Frasnian argillite interval positioned between the Bahram Formation and Permian Jamal Formation shows two disconformities at the base and top. These disconformities represent gaps of late Givetian age at the base and the Late Devonian to Carbonferous age at the top respectively.

ACKNOWLEDGEMENTS

Authors express sincerely gratitude to Drs. S. Gouwy, G.L. Albanesi and M.J. Gómez for their critical comments on the early version of the paper. We would like to express our thanks to some friends such as M.K. Kamali, F. Amin-Nezhad and Z. Shojaei who helped us in the field sampling and laboratory processing. A. Shahvaladian and H. Shafiei assisted us in transportation of the samples. This paper is financially and officially supported by the Deputy of Research and Technology, University of Hormozgan (Project no. 96/200/170).

REFERENCES

Adhamian, A. 2003. Middle Devonian (Givetian) conodont biostratigraphy in the Soh area, north of Esfahan, Iran. *Courier Forschungsinstitut Senckenberg*, **245**:183–193.

Ashouri, A.R. 2004. Late Devonian and Middle–Late Devonian conodont from eastern and northern Iran. *Revista Española de Micropaleontología*, **36**:355–365.

Bahrami, A.; Gholamalian, H.; Corradini, C. & Yazdi, M. 2011. Upper Devonian conodont biostratigraphy of Shams-Abad section, Kerman Province, Iran. *Rivista Italiana di Paleontologia e Stratigrafia*, **117**:199–209.

Bahrami, A.; Königshof, P.; Boncheva, I.; Tabatabaei, M.S.; Yazdi, M. & Safari, Z. 2015. Middle Devonian (Givetian) conodonts from the northern margin of Gondwana (Soh and Natanz regions, north-west Isfahan, Central Iran): biostratigraphy and palaeoenvironmental implications. *Palaeobiodiversity Palaeoenvironment*, **95**:555–577. *doi:10.1007/s12549-015-0205-0*

Bahrami, A.; Königshof, P.; Boncheva, I.; Yazdi, M.; Ahmadi Nahre Khalaji, M. & Zare, E. 2018. Conodont biostratigraphy of the Kesheh and Dizlu sections, and the age range of the Bahram Formation in central Iran. *Palaeobiodiversity and Palaeoenvironment*, **98**:315–329. *doi:10.1007/s12549-017-0307-y*

Barskov, I.S.; Vorontsova, T.N.; Kononova, L.I. & Kuzmin, A.V. 1991. *Oprdelitel konodontov devona i nizhnego karbona*. Moscow, Moskovskiy Gosudarstvennyy University, 183 p.

Bassler, R.S. 1925. Classification and stratigraphic use of conodonts. *Geological Society of America Bulletin*, **36**:218–220.

Belka, Z.; Kaufmann, B. & Bultynck, P. 1997. Conodont-based quantitative biostratigraphy for the Eifelian of the eastern Anti-Atlas, Morocco. *Geological Society of America Bulletin*, **109**:643–651.

Branson, E.B. & Mehl, M.G. 1938. Conodonts from the Lower Mississippian of Missouri. *In*: *Stratigraphy and paleontology of the Lower Mississippian of Missouri*, University of Missouri Studies, p. 128–148.

Brice, D.; Yazdi, M.; Torabi, H. & Maleki, A. 2006. Devonian brachiopods from the Zefreh section (Central Iran). *Annales de la Sociéte Géologique du Nord*, **13**:141–155.

Bultynck, P. 1970. Révision stratigraphique et paléontologique (Brachiopodes et Conodontes) de la coupe type du Couvinien. *Mémoires de l'Institut Géologique de l'Université de Louvain*, **26**:1–152.

Bultynck, P. 2003. Devonian Icriodontidae: biostratigraphy, classification and remarks on paleoecology and dispersal. *Revista Española de Micropaleontología*, **35**:295–314.

Dzik, J. 1976. Remarks on the evolution of Ordovician conodonts. *Acta Palaeontologica Polonica*, **21**:395–455.

Ghobadi Pour, M.; Popov, L.; Hosseini, M.; Adhamian, A. & Yazdi, M. 2013. Late Devonian (Frasnian) trilobites and brachiopods from the Soh area, Central Iran. *Memoirs of the Association of Australasian Palaeontologists*, **44**:149–158.

Gholamalian, H. 2006. Biostratigraphy of Late Devonian sequence in Hutk section (north of Kerman) based on conodonts. *Geosciences Quarterly Journal*, **59**:94–101.

Gholamalian, H.; Ghorbani, M. & Sajadi, S.H. 2009. Famennian conodonts from Kal-e-Sardar section, eastern Tabas, Central Iran. *Rivista Italiana di Paleontologia e Stratigrafia*, **115**:141–158.

Gholamalian, H.; Ghoreishi Maremy, S. & Parvaneh-Nezhad Shirazi, M. 2014. Biostratigraphy of Late Devonian Conodonts in Gerik Section, Eastern Zarand (Kerman Province). *Geosciences Scientific Quarterly Journal*, **92**:105–114.

Gholamalian, H.; Hairapetian, V.; Barfehei, N.; Mangelian, S. & Faridi, P. 2013. Givetian–Frasnian boundary conodonts from Kerman Province, Central Iran. *Rivista Italiana di Paleontologia e Stratigrafia*, **119**:141–158.

Gholamalian, H.; Hosseini-Nezhad, S.M.; Khosravi, Z. & Turkzadeh-Mahani, I. 2011. Late Devonian conodonts from Baghin section, West of Kerman. *Geosciences Quarterly Journal*, **21**:165–172.

Gholamalian, H. & Kebriaei, M.R. 2008. Late Devonian conodonts from Hojedk section, Kerman province, southeastern Iran. *Rivista Italiana di Paleontologia e Stratigrafia*, **114**:171–181.

Gouwy, S.; Liao, J.C. & Valenzuela-Ríos, J.I. 2013. Eifelian (Middle Devonian) to Lower Frasnian (Upper Devonian) conodont biostratigraphy in the Villech section (Spanish Central Pyrenees). *Bulletin of Geosciences*, **88**:315–338. *doi:10.3140/bull.geosci.1341*

Gouwy, S.; Liao, J.C. & Valenzuela-Ríos, J.I. 2016. Graphic correlation of the Upper Eifelian to Lower Frasnian (Middle-Upper Devonian) conodont sequences in the Spanish Central Pyrenees and comparison with composite standards from other areas. *Palaeontologia Electronica*, **19.3.39A**:1–18. *doi:10.26879/669*

Hairapetian, V.; Blom, H. & Turner, S. 2016. Early Frasnian thelodont scales from central Iran and their implications for turiniid taxonomy, systematics and distribution. *Journal of*

Vertebrate Paleontology, **36**:e1100632. *doi:10.1080/02724634.2016.1100632*

Hinde, G.J. 1879. On conodonts from the Chazy and Cincinnati Group of the Cambro-Silurian, and from the Hamilton and Genesee-Shale division of the Devonian, in Canada and the United States. *Geological Society of London*, *Quarterly Journal*, **35**:351–369.

Klapper, G. 1989. The Montagne Noire Frasnian (Upper Devonian) conodont succession. *In*: N.J. McMillan; A.F. Embry & D.G. Glass (eds.) *Proceedings of the Second International Symposium on the Devonian System*, Canadian Society of Petroleum Geologists, vol. 3, p. 449–468.

Klapper, G. & Johnson, J.G. 1980. Endemism and dispersal of Devonian conodonts. *Journal of Paleontology*, **54**:400–455.

Klapper, G. & Johnson, J.G. 1990. Revisions of Middle Devonian conodont zones. *In*: J.G. Johnson (ed.) *Lower and Middle Devonian brachiopod-dominated communities of Nevada*, *and their position in a biofacies-province-realm model*, *Journal of Paleontology*, **64**: 934–941.

Königshof, P.; Carmichael, S.K.; Waters, J.; Jansen, U.; Bahrami, A.; Boncheva, I. & Yazdi, M. 2017. Palaeoenvironmental study of the Palaeotethys Ocean: the Givetian-Frasnian boundary of a shallow-marine environment using combined facies analysis and geochemistry (Zefreh Section/Central Iran). *Palaeobiodiversity Palaeoenvironment*, **97**:517–540. *doi:10.1007/s12549-016-0253-0*

Molaei, H. & Torshizian, H. 2007. Study of geology, mineralogy and geotectonics of Gushkamar Bauxite, Ozbak-Kuh, East of Iran. *Research Journal of University of Esfahan*, **27**:69–86.

Narkiewicz, K. & Bultynck, P. 2007. Conodont biostratigraphy of shallow marine Givetian deposits from the Radom–Lublin area, SE Poland. *Geological Quarterly*, **51**:419–442.

Narkiewicz, K. & Königshof, P. 2018. New Middle Devonian conodont data from the Dong Van area, NE Vietnam (South China Terrane). *Paläontologische Zeitschrift*, **92**:633–650. *doi:10.1007/s12542-018-0408-6*

Nasehi, E. 1997. Early to Middle Devonian conodonts from Central Iran. *Geosciences Quarterly Journal*, **6**:78–87.

Nasehi, E. 2018. New biostratigraphical findings on the Padeha Formation based on conodont accumulation in Yazdanshahr, Kerman, Central Iran. *Applied Economic Environmental Research*, **16**:993–1018.

Müller, K.J. & Müller, E.M. 1957. Early Upper Devonian (Independence) conodonts from Iowa, Part 1. *Journal of Paleontology*, **31**:1069–1108.

Rahmati, S. & Yazdi, M. 2008. Introduction of Middle to Upper Devonian index microfossils from Soh section, North of Esfahan. *Proceeding of the 2nd symposium of Iranian Palaeontological Society*, 1–4.

Stauffer, C.R. 1938. Conodonts of the Olentangy shale. *Journal of Paleontology*, **12**:411–443.

Stauffer, C.R. 1940. Conodonts from the Devonian and associated clays of Minnesota. *Journal of Paleontology*, **14**:417–435.

Walliser, O.H.; Bultynck, P.; Weddige, K.; Becker, R.T. & House, M.R. 1995. Definition of the Eifelian - Givetian Stage boundary. *Episodes*, **18**:107–115.

Weddige, K. 1977. Die Conodonten der Eifel-Stufe im Typusgebiet und in benachbarten Faziesgebieten. *Senckenbergiana Lethaea*, **58**:271–419.

Weddige, K. 1984. Zur Stratigraphie and Palaeogeographie des Devons und Carbons von NE-Iran. *Senckenbergiana Lethaea*, **65**:179–223.

Wendt, J.; Kaufmann, B.; Belka, Z.; Farsan, N. & Karimi Bavandpour, A. 2002. Devonian/Lower Carboniferous stratigraphy, facies patterns and palaeogeography of Iran, part I, southeastern Iran. *Acta Geologica Polonica*, **52**:129–168.

Wendt, J.; Kaufmann, B.; Belka, Z.; Farsan, N. & Karimi Bavandpour, A. 2005. Devonian/Lower Carboniferous stratigraphy, facies patterns and palaeogeography of Iran, part II, northern and central Iran. *Acta Geologica Polonica*, **55**:31–97.

Yazdi, M. 1999. Late Devonian - Carboniferous conodonts from eastern Iran. *Rivista Italiana di Paleontologia e Stratigrafia*, **105**:167–195.

Yazdi, M.; Meysami A.; Mannani M.; Bakhshaei M.H. & Mawson R. 2000. Famennian conodonts from the Esteghlal Refractories Mine, Abadeh area, south-central Iran. *Records of Western Australian Museum*, *Supplement*, **58**:197–209.

Zahedi, M. 1973. Geological map of the Soh area, West Central Iran (scale 1/100000). *Geological Survey of Iran Reports*, **27**:1–197.

Ziegler, W. & Sandberg, C.A. 1990. Late Devonian standard conodont zonation. *Courier Forschungsinstitut Senckenberg*, **121**:1–115.

Received in 21 March, *2021; accepted in 09 August*, *2021*.